Publications of the Astronomical Society of the Pacific
104: 1205–1215, 1992 December

Photometry of RR Lyrae Variables in the Globular Clusters M5 and M92

J. G. COHEN

Palomar Observatory, Mail Code 105-24, California Institute of Technology, Pasadena, California 91125
Electronic mail: jlc@deimos.caltech.edu

K. MATTHEWS

Palomar Observatory, Mail Code 320-47, California Institute of Technology, Pasadena, California 91125
Electronic mail: kym@tacos.caltech.edu

Received 1992 March 10; accepted 1992 August 25

ABSTRACT. Visual photometry at V and i has been obtained for five RR Lyrae variables in the extremely metal-poor globular cluster M92 and eight in the cluster M5, of intermediate metallicity, for use in a Baade–Wesselink analysis. The periods of these variables have been updated by combining observations of the current epoch with older data from the literature. Mean magnitudes are derived from the light curves. Infrared photometry at J and K has also been obtained for two RR Lyrae variables in M92 and for four variables in the cluster M5. The data were obtained with a 58×62 pixel InSb array. The reduction and analysis techniques are discussed. Preliminary distance determinations using the $\langle M_V\rangle-$[Fe/H] relationship from the literature were derived as $(m-M)_0=14.48\pm0.04$ for M92 and 14.25 ± 0.05 for M5, while preliminary distance determinations using the $\langle M_K\rangle-\log(P)$ relationship were derived as 0.15 mag smaller.

1. INTRODUCTION

We present visual photometry for five RR Lyrae variables in the extremely metal-poor globular cluster M92 and eight in the intermediate-metallicity cluster M5. Infrared photometry is presented for two RR Lyraes in M92 and four in the globular cluster M5. These data form the basis for a Baade–Wesselink analysis of the distance to these globular-cluster variables in Cohen (1992). The large difference in metallicity between M92 and M5 will be important in efforts to understand the dependence of mean absolute V magnitude of the variables on metallicity, and to see if the globular-cluster stars obey the same relationships that prevail among the field RR Lyraes.

In addition, the globular-cluster RR Lyrae variables are of interest in their own right, as examples of high-precision light curves, for studying the bump in the light curve near phase ≈0.7, for period-shift analyses (see, e.g., Sandage 1990), and for studying possible period changes.

The advantages of infrared photometry in carrying out a Baade–Wesselink method have been amply discussed by Jameson et al. (1987) and by Jones et al. (1988). To summarize briefly, in addition to reducing the impact of any interstellar reddening, the use of K, a color far out on the Rayleigh–Jeans tail, reduces the sensitivity of the emitted flux to gravity, metallicity, and the influence of shock waves. In addition, the $(V-K)$ color offers a very broad wavelength baseline so that $T_{\rm eff}$ can be determined very reliably.

In this paper, since infrared photometry of variable stars with infrared array detectors is still relatively new, we present the data, discuss the data analysis and some of the sources of error, and give the derived mean light curve parameters.

We have two stars, one in each of the clusters, in common with the recent analysis of Storm et al. (1992), who have also embarked on a similar program. In the visual, we have four variables in common with the study of Carney et al. (1992) of M92, and five in common with Storm et al.'s (1991) analysis of M5.

2. OBSERVATIONS

2.1 Instrumental Parameters

The visual photometry was obtained with the 60-in. telescope at Palomar Mountain on the six nights of 1989 June 16–17 and 1989 June 20–23. Five of these were simultaneous with the infrared photometry obtained on the 200-in. Hale telescope described later. The visual data were obtained with a direct imaging CCD at the Cassegrain focus using interference filters designed to match the Johnson V filter and the i filter of the Thuan–Gunn (1976) system, which has $\lambda_{\rm eff}\approx8100$ A. A 800×800 pixel TI CCD was used, binned to 400×400 pixels, to give a scale of 0.48 arcsec pixel^{-1}. The output was digitized to two electrons DN^{-1}, with a ten-electron readout noise. The seeing was good; 1–1.5 arcsec every night except the last, when it was 2 arcsec. Four of the nights were photometric; two nights were cirrusy, and there was one where several hours were lost to smoke from a forest fire. Although not all the nights were photometric, local standards in each field could be used to tie the magnitudes of each frame together.

There were two CCD fields studied in M5, with the second being closer to the center of the cluster and hence more crowded, and one in M92. Exposures of 30 s in length for the M5 fields, and 40 s for the M92 field were used.

TABLE 1
Ephemerides of M5 and M92 RR Lyrae Variables

Name	Period	Zero phase (Julian Days)	Beta (days/10^6 yr)	Notes
Field 1 of M5				
M5-V32	0.45778654	2,446,536.587		
M5-V8	0.5462390	2,447,693.443	0.16	
M5-V31	0.30058294	2,446,536.731		RRc
M5-V28	0.5439272	2,446,536.666		
M5-V18	0.464233	2,447,693.519		
Field 2 of M5				
M5-V59	0.5420257	2,446,536.791		
M5-V12	0.467704	2,447,693.133	-0.21	
M5-V79	0.33313838	2,446,536.814		RRc
M92 Field				
M92-V1	0.7027955	2,447,693.233		
M92-V2	0.6438847	2,427,693.458		
M92-V6	0.599999	2,447,693.510		
M92-V10	0.3772990	2,447,693.492		Blashko, RRc
M92-V5	0.6196639	2,447,693.231		

TABLE 2
Light curves of M92 Variables at V

Phase	M92-V1	M92-V2	M92-V5	M92-V6	M92-V10
0.00	14.60	14.55	14.58	14.41	14.95
0.02	14.64	14.56	14.60	14.47	14.95
0.04	14.69	14.62	14.64	14.53	14.96
0.06	14.72	14.67	14.68	14.57	14.96
0.08	14.77	14.73	14.75	14.63	14.97
0.10	14.81	14.78	14.82	14.67	14.99
0.12	14.84	14.83	14.87	14.73	15.00
0.14	14.86	14.88	14.90	14.77	15.02
0.16	14.87	14.94	14.96	14.82	15.03
0.18	14.88	14.96	14.99	14.86	15.06
0.20	14.89	14.98	15.01	14.89	15.09
0.22	14.91	15.02	15.07	14.93	15.10
0.24	14.93	15.04	15.10	14.97	15.13
0.26	14.96	15.06	15.12	15.02	15.15
0.28	15.00	15.09	15.13	15.04	15.17
0.30	15.05	15.12	15.14	15.07	15.19
0.32	15.09	15.15	15.15	15.09	15.21
0.34	15.11	15.18	15.16	15.14	15.24
0.36	15.15	15.21	15.19	15.18	15.28
0.38	15.18	15.21	15.23	15.22	15.31
0.40	15.20	15.22	15.24	15.24	15.32
0.42	15.22	15.25	15.29	15.27	15.36
0.44	15.23	15.26	15.32	15.30	15.37
0.46	15.24	15.30	15.36	15.32	15.38
0.48	15.26	15.32	15.37	15.34	15.39
0.50	15.27	15.36	15.40	15.35	15.40
0.52	15.28	15.39	15.38	15.35	15.41
0.54	15.29	15.40	15.39	15.36	15.44
0.56	15.30	15.41	15.41	15.36	15.45
0.58	15.32	15.42	15.41	15.36	15.44
0.60	15.31	15.42	15.41	15.36	15.43
0.62	15.31	15.41	15.42	15.39	15.44
0.64	15.31	15.41	15.41	15.42	15.43
0.66	15.31	15.41	15.42	15.45	15.43
0.68	15.31	15.41	15.42	15.47	15.42
0.70	15.33	15.38	15.42	15.46	15.40
0.72	15.34	15.37	15.40	15.47	15.38
0.74	15.35	15.33	15.40	15.46	15.35
0.76	15.36	15.35	15.43	15.45	15.30
0.78	15.38	15.37	15.46	15.42	15.25
0.80	15.41	15.41	15.50	15.40	15.20
0.82	15.43	15.43	15.48	15.41	15.15
0.84	15.45	15.45	15.51	15.42	15.10
0.86	15.45	15.46	15.53	15.44	15.07
0.88	15.40	15.43	15.55	15.45	15.04
0.90	15.30	15.40	15.48	15.40	15.02
0.92	15.10	15.27	15.29	15.24	15.00
0.94	14.88	15.05	15.01	14.89	14.97
0.96	14.77	14.87	14.78	14.72	14.96
0.98	14.66	14.65	14.63	14.47	14.95

TABLE 3
Light curves of M92 Variables at i

Phase	M92-V1	M92-V2	M92-V5	M92-V6	M92-V10
0.00	14.91	14.90	14.91	14.85	15.24
0.02	14.93	14.91	14.92	14.88	15.25
0.04	14.95	14.94	14.95	14.92	15.26
0.06	14.98	14.97	14.99	14.96	15.26
0.08	15.00	15.01	15.05	14.97	15.27
0.10	15.02	15.04	15.10	14.99	15.28
0.12	15.03	15.07	15.13	15.02	15.30
0.14	15.03	15.10	15.16	15.04	15.31
0.16	15.04	15.14	15.18	15.06	15.33
0.18	15.05	15.17	15.20	15.08	15.34
0.20	15.07	15.18	15.21	15.10	15.35
0.22	15.08	15.19	15.23	15.11	15.35
0.24	15.09	15.20	15.25	15.14	15.36
0.26	15.10	15.20	15.26	15.16	15.37
0.28	15.11	15.21	15.26	15.18	15.38
0.30	15.13	15.22	15.25	15.19	15.39
0.32	15.15	15.23	15.24	15.21	15.42
0.34	15.18	15.23	15.24	15.24	15.43
0.36	15.21	15.23	15.25	15.26	15.44
0.38	15.23	15.24	15.28	15.29	15.46
0.40	15.25	15.24	15.30	15.31	15.47
0.42	15.26	15.24	15.34	15.32	15.49
0.44	15.27	15.25	15.36	15.33	15.51
0.46	15.27	15.28	15.39	15.34	15.52
0.48	15.27	15.29	15.41	15.36	15.53
0.50	15.28	15.31	15.42	15.38	15.54
0.52	15.28	15.35	15.42	15.40	15.55
0.54	15.30	15.38	15.43	15.41	15.56
0.56	15.31	15.39	15.44	15.41	15.56
0.58	15.33	15.40	15.44	15.42	15.55
0.60	15.32	15.40	15.45	15.42	15.55
0.62	15.32	15.40	15.45	15.43	15.55
0.64	15.31	15.40	15.45	15.44	15.56
0.66	15.32	15.39	15.46	15.46	15.55
0.68	15.33	15.35	15.47	15.49	15.54
0.70	15.35	15.36	15.47	15.50	15.54
0.72	15.36	15.34	15.47	15.50	15.53
0.74	15.37	15.33	15.47	15.51	15.52
0.76	15.38	15.33	15.50	15.51	15.50
0.78	15.40	15.38	15.53	15.50	15.47
0.80	15.43	15.41	15.56	15.48	15.45
0.82	15.46	15.44	15.58	15.49	15.40
0.84	15.47	15.47	15.60	15.50	15.37
0.86	15.49	15.51	15.61	15.50	15.34
0.88	15.46	15.50	15.62	15.50	15.32
0.90	15.43	15.48	15.55	15.51	15.30
0.92	15.22	15.40	15.40	15.43	15.28
0.94	15.09	15.23	15.23	15.25	15.26
0.96	15.06	15.13	15.12	15.03	15.25
0.98	14.96	14.96	14.99	14.90	15.24

This gave a net count rate for a M92 RR Lyrae of 35,000 DN at V, with the sky contributing about 250 DN pixel^{-1} at i, somewhat less than this at V. Over the 6 nights of observation there are about 350 V frames and about 300 i frames of M92, and about 100 V frames and 80 i frames for each of the 2 fields covered in M5.

2.2 Data Analysis of the Visual Photometry

First all the frames were flattened using standard techniques with dome flat fields taken before and after each night's observing. All the frames of a given field were then shifted by an integer number of pixels in x and y so that the fields are aligned to overlie each other. Since the cluster fields are rather crowded, they were analyzed using the profile fitting routine PEAK of DAOPHOT (Stetson 1987). (The crowding was not so bad that the full capability of DAOPHOT's multiple overlapping stellar profile fitting routine NSTAR was felt necessary.) Since these frames were analyzed in as automatic a manner as possible, there may

be rare cases of overlapping defects, cosmic rays, and other such that have not been weeded out manually.

The variables on each of the frames were analyzed differentially relative to a set of from 10 to 16 uncrowded bright stars on each field. The differential comparisons yielded the number of stars matched up (not the full complement, because often some stars shifted off the edge of the frame during the alignment process), the mean difference in the PEAK magnitudes between the differential standards on the frame and on the adopted calibration list, and the rms dispersion about that mean. When the frames are correctly aligned relative to each other, $\sigma=0.02$ to 0.04 mag for 12 stars. This procedure yielded magnitudes of the RR Lyrae variables relative to the differential standards. In the case of a few M92 variables near the edges of the frames, perfect alignment of the frames was sometimes not achieved, and the magnitudes show a larger than expected scatter.

The magnitudes are calibrated to those of the photometric standards observed on the night of 1989 June 23. Six standard stars from the list of Thuan and Gunn were observed at V, and there are nine standard star observations at i. Visual inspection of the field of each star on the list of differential standards for nearby neighbors produced a shorter list of completely uncrowded bright differential standard stars. In the numbering system of Arp (1962), they are M5 IV-26, IV-88, IV-80, IV-85, IV-87, and IV-86 for the first M5 field, and III-2, III-16, III-15, II-16, III-6, III-26, III-12, and III-9 for the second M5 field. For M92, the standards were I-28, II-104, XII-34, and XII-45 in the numbering system of Sandage and Walker (1966). Large aperture photometry was carried out using Figaro for each of these to define the aperture growth curve and hence the aperture correction, and the combination of these, the Palomar standard extinction coefficients, and their DAOPHOT PEAK magnitudes defined the relative calibration to the bright photometric standards. The visual photometry of the M5 and M92 RR Lyraes is given in Tables A1 to A6.

2.3 Comparison with Previous Visual Photometry

For M92, much of the published photometry is analysis of very deep CCD studies of small fields, and is not relevant here. Comparison of the four standard stars between our measurements and those of Sandage and Walker (1966) gives a small systematic difference between Sandage and Walker's magnitudes and the present ones of $\delta(V)=-0.03$ mag, with $\sigma=0.09$ mag. Comparison over the full set of our differential standards yields a mean difference of -0.16 mag with $\sigma=0.08$ mag. It appears that Sandage and Walker may have had a magnitude dependent scale error, larger at fainter magnitudes. This effect was already noted by Buonanno et al. (1983). Our agreement with the photographic study of Buonanno et al. (1983) is gratifying; for our nine differential standard stars there is a mean difference of 0.00 mag with $\sigma=0.04$ mag.

For M5, there is a photographic study by Buonanno et al. (1981) using Arp's (1962) photoelectric calibration. For six differential standard stars in field 1, the mean difference is 0.03 ± 0.02, while for the more crowded field 2, the agreement is worse, for eight stars it is 0.09 ± 0.04. In both cases our V magnitudes are systematically brighter. Richer and Fahlman (1987), in a very deep color–magnitude study of M5, found their V magnitudes to be systematically 0.06 ± 0.07 brighter than Buonanno et al.'s. Thus comparison with previous photometry of M5 indicates that agreement with the most reliable previous photometry is good, and our magnitude scale is correct.

3. RESULTS

3.1 RR Lyrae Periods and Phases

Five RR Lyrae variables in M92 were studied. Their positions relative to the cluster center are given in Sawyer Hogg (1973). The initial guesses at period and phase were taken from Kukharkin and Kukharkina (1980), or, for M92 V6, which was not included in that work, from Sawyer Hogg (1973). The periods needed updating in most cases, as manifested by small shifts in phase. The periods were corrected by using the published period as an initial guess, and forcing an integral number of cycles to have elapsed between the zero phase determined from the 1989 June data and the previous epoch of observation. The adopted periods, rate of change of the period (dP/dt), and phase zero points are listed in Table 1.

Kukharkin and Kukharkina (1980) gave an extensive discussion of the variation of period of these RR Lyrae variables in M92 with epoch of observation. They found many abrupt period changes, but no firm case of a secularly changing period. We find two cases where the period decreased in the recent past, and three where it increased. As might be expected, there is good agreement between our new periods and those calculated by Carney et al. (1992).

For M5, we repeated the same two fields used by Cohen and Gordon (1987), which cover 8 RR Lyraes. Their phases and periods were used as initial guesses. They were adequate for all the M5 variables except M5 V8, V12, and V18, where apparently period changes have occurred since 1986.

Coutts and Sawyer Hogg (1969) have given an extensive discussion of period shifts among the M5 RR Lyraes with data reaching back to 1889. They claim that V18 is too irregular to derive a period shift. We agree; the period changed by so much that the phase was off between 1986 and 1989 by 0.32 cycles. Coutts and Sawyer Hogg believe that the period of M5–V8 is increasing with time. We concur. Similarly, they believe M5–V12 has a decreasing period. Again we concur. But the period differences we derive over the three-year time baseline are about a factor of 2 larger than would be predicted by their coefficients for the rate of change of the period (dP/dt) for these two stars.

3.2 Mean Magnitudes

As the visual photometry is very extensive and of high accuracy, we give the mean V and i light curves for the RR Lyraes in M92 in Tables 2 and 3, and the mean light curves for the RR Lyraes in M5 are given in Tables 4 and 5.

TABLE 4
Light curves of M5 Variables at V

Phase	M5-V8	M5-V12	M5-V18	M5-V28	M5-V31	M5-V32	M5-V59	M5-V79
0.00	14.530	14.330		14.560	14.880	14.290		14.810
0.02	14.590	14.410		14.580	14.870	14.310		14.810
0.04	14.620	14.460		14.620	14.880	14.350		14.810
0.06	14.640	14.520	14.740	14.680	14.890	14.420		14.830
0.08	14.670	14.580	14.770	14.740	14.900	14.490		14.860
0.10	14.700	14.650	14.800	14.790	14.920	14.560		14.870
0.12	14.740	14.700	14.840	14.840	14.930	14.620		14.880
0.14	14.810	14.770	14.910	14.860	14.940	14.680		14.890
0.16	14.920	14.840	14.980	14.890	14.960	14.750		14.900
0.18	14.960	14.900	14.990	14.940	14.980	14.800		14.900
0.20	14.980	14.940	15.050	14.970	15.000	14.840		14.910
0.22	15.030	14.980	15.090	15.000	15.010	14.910		14.940
0.24	15.070	15.020	15.130	15.030	15.030	14.960		14.960
0.26	15.120	15.050	15.160	15.050	15.050	15.000	14.920	
0.28	15.160	15.086	15.180	15.080	15.070	15.040	14.920	
0.30	15.190	15.122	15.220	15.110	15.090	15.080	14.940	
0.32	15.210	15.158	15.270	15.150	15.130	15.120	14.970	
0.34	15.230	15.194	15.300	15.190	15.160	15.160	15.000	
0.36	15.240	15.230	15.320	15.210	15.180	15.200	15.060	
0.38	15.270	15.260	15.340	15.240	15.210	15.230	15.120	
0.40	15.300	15.290	15.360	15.260	15.240	15.250	15.150	
0.42	15.330	15.320	15.380	15.290	15.280	15.290	15.160	
0.44	15.360	15.350	15.410	15.320	15.300	15.320	15.190	
0.46	15.360	15.380	15.400	15.330	15.320	15.340	15.210	
0.48	15.370	15.405	15.420	15.350	15.350	15.360	15.190	
0.50	15.380	15.430	15.440	15.360	15.340	15.380	15.200	
0.52	15.390	15.455	15.460	15.360	15.360	15.410	15.220	
0.54	15.390	15.480	15.490	15.370	15.370	15.450	15.240	
0.56	15.400	15.500	15.490	15.380	15.370	15.470	15.240	
0.58	15.400	15.505	15.480	15.370	15.370	15.480	15.210	
0.60	15.410	15.510	15.470	15.370	15.360	15.460	15.210	
0.62	15.400	15.513	15.500	15.380	15.350	15.450	15.220	
0.64	15.410	15.515	15.530	15.390	15.310	15.440	15.230	
0.66	15.420	15.520	15.500	15.390	15.310	15.420	15.240	15.090
0.68	15.430	15.530	15.490	15.390	15.320	15.440	15.240	15.060
0.70	15.450	15.533	15.490	15.400	15.320	15.440	15.240	15.010
0.72	15.480	15.536	15.540	15.400	15.310	15.450	15.250	14.980
0.74	15.520	15.539	15.530	15.400	15.290	15.460	15.240	14.950
0.76	15.530	15.542	15.530	15.400	15.250	15.470	15.260	14.930
0.78	15.540	15.545	15.500	15.400	15.200	15.460	15.290	14.900
0.80	15.550	15.548	15.470	15.420	15.150	15.440	15.320	14.880
0.82	15.560	15.551	15.460	15.460	15.080	15.460	15.350	14.870
0.84	15.570	15.554	15.420	15.460	14.990	15.490	15.350	14.850
0.86	15.510	15.557	15.340	15.460	14.920	15.540	15.370	14.840
0.88	15.160	15.515	15.140	15.370	14.910	15.590	15.390	14.830
0.90	15.000	15.460	15.000	15.260	14.900	15.560	15.320	14.820
0.92	14.920	15.340	14.930	15.100	14.880	15.460	15.180	14.800
0.94	14.800	14.950		14.970	14.890	15.240	15.010	14.800
0.96	14.690	14.620		14.870	14.880	14.880		14.800
0.98	14.590	14.430		14.670	14.880	14.460		14.800

TABLE 5
Light curves of M5 Variables at i

Phase	M5-V8	M5-V12	M5-V18	M5-V28	M5-V31	M5-V32	M5-V59	M5-V79
0.00	14.82	14.830		14.890	15.170	14.720		15.060
0.02	14.85	14.860		14.910	15.190	14.750		15.065
0.04	14.89	14.890		14.930	15.200	14.780		15.070
0.06	14.91	14.920	15.040	14.970	15.210	14.830		15.060
0.08	14.93	14.960	15.070	15.010	15.210	14.880		15.070
0.10	14.95	15.015	15.090	15.030	15.220	14.920		15.080
0.12	14.98	15.045	15.120	15.040	15.220	14.960		15.090
0.14	15.00	15.080	15.150	15.050	15.220	14.990		15.090
0.16	15.02	15.120	15.170	15.080	15.230	15.030		15.100
0.18	15.04	15.140	15.180	15.090	15.240	15.070		15.110
0.20	15.06	15.170	15.200	15.100	15.260	15.110		15.110
0.22	15.08	15.190	15.250	15.120	15.270	15.150		
0.24	15.11	15.210	15.280	15.140	15.280	15.170	15.020	
0.26	15.13	15.230	15.260	15.150	15.290	15.200	15.040	
0.28	15.17	15.250	15.280	15.170	15.300	15.220	15.050	
0.30	15.18	15.270	15.300	15.180	15.310	15.250	15.060	
0.32	15.20	15.292	15.330	15.190	15.320	15.270	15.080	
0.34	15.22	15.314	15.340	15.200	15.350	15.290	15.090	
0.36	15.24	15.336	15.360	15.210	15.390	15.310	15.110	
0.38	15.25	15.358	15.380	15.230	15.410	15.330	15.130	
0.40	15.27	15.380	15.400	15.240	15.420	15.360	15.150	
0.42	15.28	15.394	15.420	15.260	15.440	15.390	15.190	
0.44	15.29	15.408	15.420	15.280	15.460	15.380	15.200	
0.46	15.31	15.422	15.420	15.300	15.470	15.400	15.220	
0.48	15.32	15.436	15.430	15.310	15.490	15.410	15.220	
0.50	15.33	15.450	15.450	15.330	15.490	15.420	15.230	
0.52	15.35	15.470	15.490	15.340	15.500	15.440	15.240	
0.54	15.36	15.500	15.500	15.340	15.510	15.450	15.260	
0.56	15.37	15.520	15.510	15.350	15.490	15.480	15.260	
0.58	15.36	15.550	15.470	15.360	15.480	15.510	15.250	
0.60	15.36	15.555	15.500	15.360	15.490	15.520	15.250	
0.62	15.37	15.560	15.500	15.370	15.490	15.510	15.260	
0.64	15.38	15.570	15.500	15.370	15.490	15.500	15.260	
0.66	15.38	15.580	15.500	15.370	15.490	15.470	15.260	15.220
0.68	15.39	15.585	15.500	15.380	15.500	15.450	15.260	15.220
0.70	15.41	15.588	15.540	15.400	15.490	15.460	15.270	15.210
0.72	15.41	15.591	15.540	15.410	15.500	15.480	15.280	15.190
0.74	15.42	15.594	15.540	15.420	15.480	15.500	15.280	15.170
0.76	15.43	15.597	15.540	15.420	15.430	15.510	15.280	15.160
0.78	15.45	15.600	15.540	15.420	15.420	15.510	15.330	15.160
0.80	15.49	15.603	15.530	15.420	15.410	15.490	15.350	15.150
0.82	15.54	15.606	15.520	15.420	15.360	15.520	15.370	15.120
0.84	15.56	15.609	15.450	15.420	15.310	15.520	15.410	15.100
0.86	15.56	15.612	15.410	15.420	15.260	15.550	15.430	15.080
0.88	15.52	15.600	15.340		15.240	15.560	15.410	15.070
0.90	15.43	15.600	15.250		15.220	15.570	15.370	15.060
0.92	15.29	15.510	15.220		15.210	15.510	15.260	15.060
0.94	15.18	15.170			15.210	15.320		15.070
0.96	15.07	14.990			15.190	15.180		15.060
0.98	14.91	14.860			15.170	14.880		15.060

Figures 1 and 2 show the V and i light curves, respectively, for the 13 RR Lyrae variables.

Table 6 contains the magnitude mean and intensity mean parameters of the light curve. No reddening corrections have been applied. M5–79 is omitted from Table 6 due to incomplete phase coverage. For the four RR Lyrae variables in M92 in common with Carney et al. (1992), we find a mean difference of 0.03 ± 0.03 for the magnitude mean V values. If the intensity mean values are compared, the difference is 0.05 ± 0.02. All the M5 stars in common with Carney et al. (1991) are in field 1. The difference of the magnitude means is 0.05 ± 0.03, while the difference of the intensity means yields 0.07 ± 0.03.

Using the data in Cohen and Gordon to supply mean magnitudes for M5–V79, we find that both c-type RR Lyrae variables in M5 are well separated from the remaining variables in a plot of $(V, V-i)$. This also holds for the only M92 c-type RR Lyrae (M92–V10). This shows that $(V-i)$ is a better indicator of $T_{\rm eff}$ than is $(B-V)$ (see Storm et al. 1991).

4. INFRARED PHOTOMETRY

4.1 Infrared Observations

Infrared photometry at J and K was obtained using the Cassegrain IR array camera on the 200-in. Hale telescope on the nights of 1989 June 16–17 and 1989 June 21–23, simultaneously with the optical photometry described above obtained on the 60-in. telescope. Only four of the five nights were photometric (the fifth suffered from moderate cirrus), and several hours were lost of another due to smoke from a nearby forest fire. Thus local standards in several of the fields had to be be used to tie the magnitudes of each frame of a particular variable together. The visual seeing was between 1.0 and 1.5 arcsec for four of the five nights and about 2.0 arcsec on the last night.

The camera contains a Hughes Santa Barbara Research Center 58×62 element InSb array, used at the $f/70$ low-background Cassegrain focus. The scale is 0.31 arcsec pixel^{-1}. The array has a dark current of 90 e pixel^{-1} s^{-1}, and a readout noise of 450 e. It is digitized to 1 DN/90 e. The array has two large cracks that one must avoid placing stellar images on or near, as well as several bad pixels. Although this was one of the earliest nonengineering runs of this camera, the array performed well and was very stable. Many subsequent experiments have shown the system to be stable in both responsivity and linearity.

It was hoped that by using an array, one could overcome two serious problems which arise in infrared photometry of globular-cluster RR Lyrae variables using single element detectors. The first is the crowding in these cluster fields, which makes observations using aperture photometry difficult unless the seeing is extremely good and stable, so that small aperture sizes can be used. The second constraint is the problem of achieving full phase coverage with a limited allocation of nights on a large telescope, some of which might be nonphotometric. It was hoped that the use of an IR array would permit the same procedure of local standards near each star used so suc-

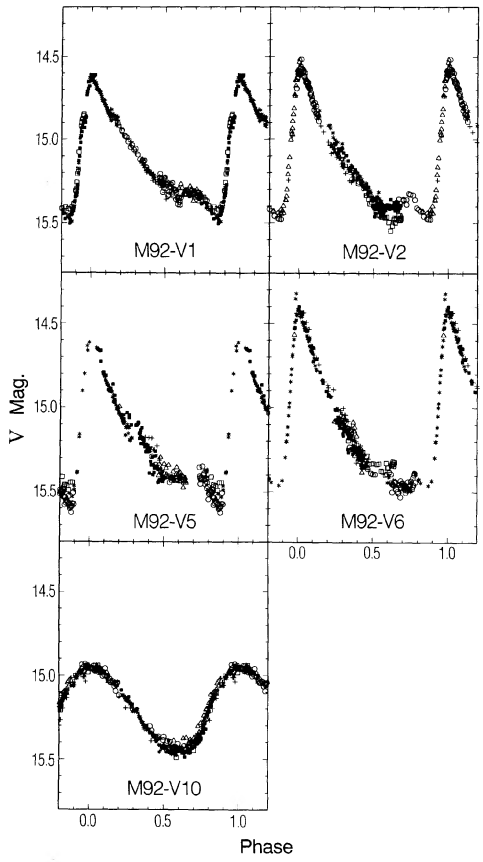

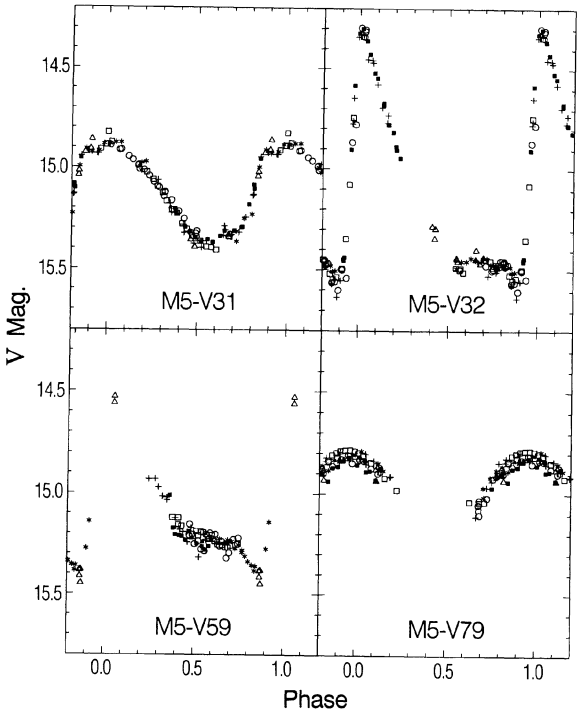

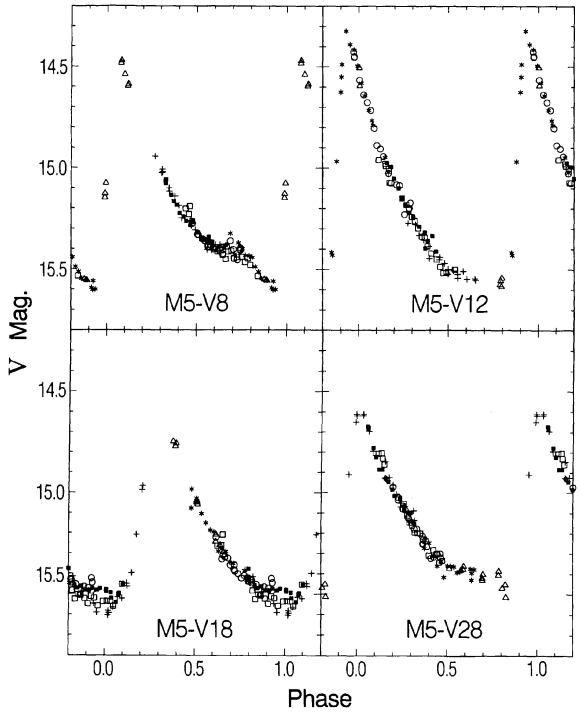

FIG. 1—The V light curves of RR Lyrae variables in M5 and M92 are shown as a function of phase. The different symbols denote different nights of observation.

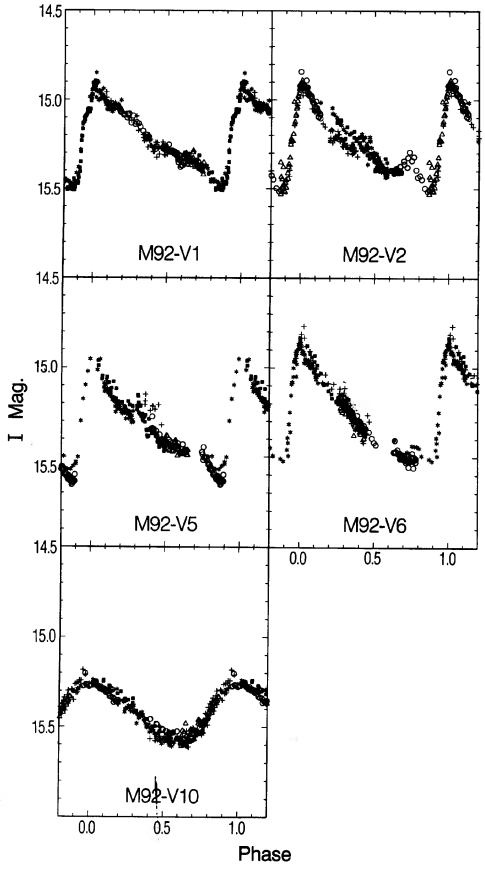

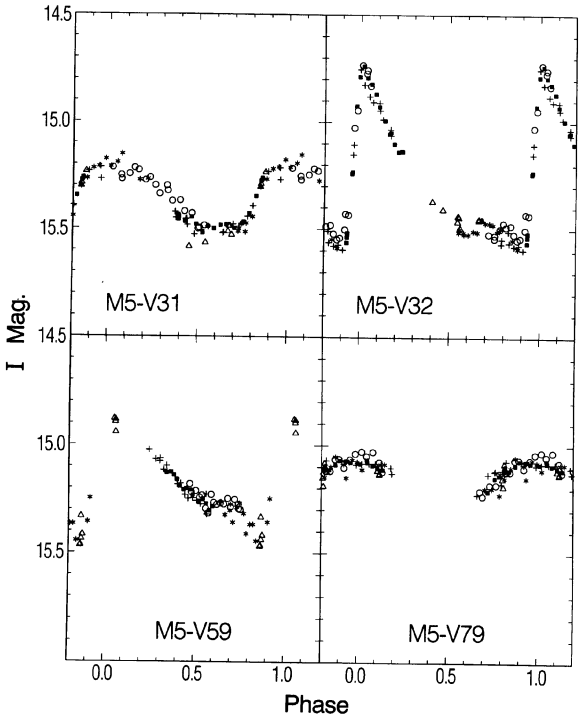

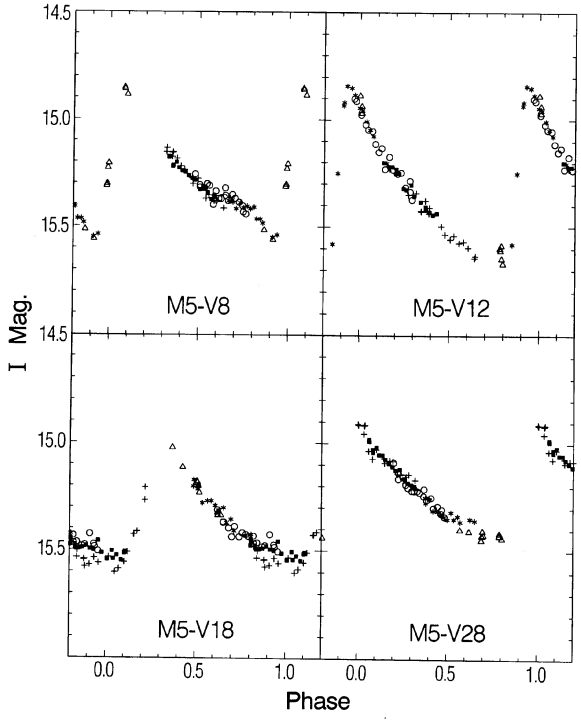

FIG. 2—The *i* light curves of RR Lyrae variables in M5 and M92 are shown as a function of phase. The different symbols denote different nights of observation.

TABLE 6
Mean Magnitudes of M92 and M5 RR Lyrae Variables

Star	$< M_V >$	$< M_{V(int)} >$	$< M_i >$	$< M_{i(int)} >$
M5-V8	15.166	15.146	15.236	15.228
M5-V12	15.184	15.154	15.340	15.327
M5-V18	15.196	15.148	15.319	15.312
M5-V28	15.158	15.143	15.225	15.220
M5-V31	15.118	15.111	15.344	15.347
M5-V32	15.143	15.113	15.290	15.277
M5-V59	15.032	15.016	15.135	15.128
M92-V1	15.119	15.107	15.213	15.208
M92-V2	15.164	15.149	15.254	15.249
M92-V5	15.192	15.176	15.320	15.313
M92-V6	15.129	15.108	15.274	15.265
M92-V10	15.202	15.195	15.412	15.409

cessfully at optical wavelengths, so that even if conditions were not ideal, useful data could still be obtained.

While the first advantage of using an array cited above was achieved, the second was only partially realized. In 1989, infrared arrays were still quite small (18×19 arcsec for the array used here), with many localized defects, so one must be quite careful where the object of interest is located if accurate photometry is desired. Hence it was only possible to define local standards around half of the variables.

Since the RR Lyraes in a given cluster are far apart compared to the field size of the IR detector, each RR Lyrae had to be imaged individually with the infrared array camera. Thus, in M92, we obtained IR photometry only for variables M92 V1 and M92 V6. In M5, the same four variables analyzed in detail by Cohen and Gordon (1987) were repeated, M5 V32, M5 V8, M5 V12, and M5 V59.

The fainter standard stars of Elias et al. (1982) were used to reproduce the CIT system. In addition to standard flat fields, dark frames and a sequence of flat fields of varying exposure times were taken at the beginning of each night. The nonlinearity of the array (about 4% over its useful dynamic range) was measured each night. Integration time for the standard stars was a sum of ten frames, each 0.25 s long. Eight to ten standard stars were observed each photometric night.

For the globular-cluster RR Lyraes, the exposure time was 20 s, except for the cirrusy night, when 30-s exposures were used. The former gave more than 3000 DN in a typical K image of a variable, and for the J image somewhat more. The sky was typically 500 DN pixel^{-1} in the J exposures, and 3500 DN pixel^{-1} in the K frames. Saturation is at more than 10,000 DN pixel^{-1}.

A measurement, either of a standard or a program star, consisted of a pair of frames, one through the J filter, and the second through the K filter. After each measurement, a second pair of frames with identical exposure times was taken with the telescope slightly shifted in position by a few arcseconds so as to move the object around on the array. The stars were moved automatically by shifting the autoguider between exposures. Thus each object always fell at one of approximately the same two positions on the array during each night. After a sequence such that all the RR Lyraes in a given cluster were observed, sky frames were taken for the RR Lyraes by moving the telescope several hundred arcseconds away to a suitable location far from the cluster center.

TABLE 7
J and K Photometry of RR Lyrae M92–V1

Geocentric Julian Date −2,447,000.0	Phase	J (mag)	K (mag)
693.740	0.721	14.116	13.925
693.788	0.789	14.159	13.936
693.826	0.843	14.180	13.987
693.860	0.893	14.193	14.033
693.903	0.953	14.035	13.998
693.915	0.970	13.923	13.858
693.928	0.990	13.966	13.905
693.942	0.009	13.917	13.897
693.958	0.031	13.856	13.837
693.971	0.050	13.882	13.827
694.656	0.024	13.987	13.670
694.688	0.071	13.915	13.661
694.717	0.111	13.981	13.785
694.751	0.161	14.057	13.795
694.788	0.213	13.939	13.701
694.835	0.279	13.822	13.643
694.872	0.332	14.005	13.812
694.886	0.352	13.965	13.834
694.897	0.368	14.136	13.813
694.908	0.384	14.180	13.808
694.919	0.400	14.162	13.857
694.931	0.415		13.791
694.943	0.433	13.889	
694.956	0.451	14.018	
694.967	0.468	13.994	
694.978	0.483	14.013	
694.989	0.498	14.208	
698.681	0.751	14.255	13.892
698.715	0.801	14.242	14.047
698.758	0.861	14.214	13.964
698.788	0.904	14.223	13.911
698.894	0.056	13.910	13.794
698.913	0.081	13.992	13.831
698.940	0.120	13.971	13.719
698.951	0.136	13.985	13.790
699.677	0.169	13.912	13.722
699.710	0.216	13.953	13.721
699.738	0.256	13.978	13.750
699.766	0.296	13.962	13.709
699.808	0.356	14.021	13.781
699.884	0.464	14.077	13.836
699.893	0.476	14.035	13.796
699.912	0.503	14.134	13.780
699.958	0.568	14.152	13.859
699.979	0.598	14.180	13.922
700.683	0.601		13.859
700.714	0.644	14.184	13.849
700.751	0.697	14.157	13.769
700.780	0.738	14.182	13.887
700.819	0.795	14.225	13.945
700.844	0.830	14.341	13.980
700.865	0.860	14.298	14.004
700.885	0.889	14.316	14.059
700.915	0.930	14.128	13.934
700.928	0.950	14.052	13.863
700.937	0.962	13.955	13.823
700.947	0.976	14.074	13.739
700.957	0.990	13.955	13.843
700.976	0.018	13.918	13.803

There are 118 observations of each M92 star and 60 of each M5 star.

4.2 Data Analysis

The IR array is slightly nonlinear. This was modeled on a global basis over the frame using a sequence of exposures of varying durations of a dome flat-field lamp. The linearity correction curve, whose maximum amplitude was about 4%, is the ratio of the actual signal in a dome flat-field exposure S_A of integration time t_A divided by the signal expected by extrapolating from a 1-s flat-field exposure S_1, $S_A/(S_1 t_A)$. This function of observed signal S_A was constant over the entire run. It was fit by a spline and the correction was applied to all pixels in each of the frames. Once the IR frames were linearized, the sky frame was subtracted from the object frame, and the difference frame was flattened. There were slight problems in flat fielding the data at J, and occasionally a coherent noise pattern (like microphonics) was seen in the flattened J frames. This never exceeded 10 DN in peak-to-peak amplitude.

Next the brightness of the object was measured using the aperture photometry code in Figaro. A 10 pixel diameter aperture, corresponding to 3.1 arcsec, was used. The variables M92–V6 and M5–V59 had adjacent reasonably bright (i.e., at lease 0.3 mag brighter than the variables at maximum light) neighbors on the same frame that could be used to define relative magnitudes, while M5–V8 had a somewhat fainter neighbor. The star 3.8-arcsec SW of M92–V6 was used to define the scale for that cluster, with $K=11.97$ mag and $J=12.54$ mag. The star M5 III-9 in the numbering system of Arp (1962), 7.8-arcsec NE of M5–V59, with $K=12.63$ mag and $J=13.20$ mag, normalizes the M5 magnitudes. The remaining variables used the magnitude offsets from whichever of these two is in the relevant cluster.

This method of removing the influence of those time-dependent effects such as extinction and seeing profiles was much more successful than just relying on the bright standard stars.

Standard Palomar airmass corrections were used. Note that the M5 observations spanned a more extreme range in airmass than did those of M92, reaching 1.9 on occasion before work on M5 was abandoned for the night.

4.3 Crowding Corrections

Only M92–V6 is sufficiently crowded for this to be a concern. There are two neighboring stars, the brighter one 3.8 arcsec to the SW, and a faint star 2.5 arcsec to the NW. The brighter star is about 1.9 mag brighter than the RR Lyrae M92–V6, while the fainter star is about 0.8 mag fainter. The growth curve for magnitude as a function of aperture size was studied for the standard stars. The correction itself, and the range of variation of M92–V6, are both sufficiently small that use of a constant crowding correction seems suitable. As a result, a uniform crowding correction of 0.03 mag was applied at J and at K to the observed photometry of M92–V6. The crowding correction is dominated by the contribution of the brighter, more distant, neighbor.

4.4 Final Magnitudes

The resulting J and K magnitudes, averaged over the pairs of frames, are given in Tables 7 and 8 for the M92 variables, and in Tables 9–12 for the M5 variables. Missing values occurred primarily for two reasons. Occasionally the filter mover software would malfunction, and the J frames of a given measurement were in fact K frames. In addition, toward the end of the second night, after M5 had already set, there was a period of rapidly fluctuating transparency. While the differential standard star on the frame of M92–V6 enabled us to retain full data coverage for that star, some K measurements for M92–V1 were disregarded. Figures 3 and 4 show the light curves for the two M92 variables, and Fig. 5 is among the better of the M5 RR Lyrae light curves in that it has relatively complete phase coverage.

Although we expected, based on the observed count rates in the objects and in the sky, to achieve a photometric accuracy of 1% at J and at K, the infrared light curves are rather ragged, and show that the accuracy achieved was significantly degraded, and is not better than 3% for each pair of measurements. Since the best light curves are those with local standards on the same frame, we believe that this is a consequence of possible small variations in atmospheric transmission, extinction deviations from the standard Palomar extinction law used, and variations in the stellar point spread function (PSF) affecting the fraction of total light included in our 3.1-arcsec aperture.

5. APPLICATION OF THE MEAN MAGNITUDES

As reviewed by Liu and Janes and by Carney et al. (1992), based on extensive Baade–Wesselink analyses of field RR Lyrae stars, these variables obey a number of well-established relationships. One of them is a relationship between absolute luminosity at V and metallicity,

$$\langle M_V \rangle = 0.20(\pm 0.07)\,[\mathrm{Fe/H}] + 1.06(\pm 0.13).$$

We apply this without justification to the globular-cluster RR Lyrae stars. We adopt reddening corrections of $E(B-V)=0.03$ for M5 (Zinn 1980) and 0.02 for M92 (Stetson and Harris 1988), with $A_V=3.1E(B-V)$. For both clusters, the reddenings are small, so the exact choice from among the large number of published values is not very important. We adopt the metallicities of Zinn (1985) to obtain for the mean of the four M92 stars a distance modulus $(m-M)_0=14.48\pm0.04$, and for seven stars in M5 we obtain $(m-M)_0=14.25\pm0.05$.

Since we intend to use these light curves of RR Lyrae variables in M5 and M92 in a subsequent paper (Cohen 1992) on the Baade–Wesselink method, we defer detailed discussion here. Instead we emphasize a second possible method of distance determination. As discussed by Liu and

TABLE 8
J and *K* Photometry of RR Lyrae M92–V6

Geocentric Julian Date −2,447,000.0	Phase	J (mag)	K (mag)
693.749	0.398	14.118	13.882
693.792	0.471	14.161	13.897
693.829	9.532	14.131	13.893
693.864	0.590	14.217	13.936
693.906	0.660	14.256	13.992
693.918	0.680	14.257	13.998
693.933	0.706	14.272	14.010
693.946	0.726	14.318	14.041
693.960	0.751	14.318	14.033
693.974	0.774	14.316	14.061
693.981	0.784	14.314	14.081
694.663	0.922	14.259	13.917
694.692	0.969	14.021	13.706
694.721	0.018	13.925	13.793
694.757	0.078	13.959	13.829
694.794	0.141	14.009	13.829
694.844	0.224	14.034	13.811
694.877	0.278	14.047	13.892
694.889	0.298	14.065	13.831
694.901	0.318	14.099	13.860
694.913	0.338	14.119	13.849
694.923	0.355	14.108	13.845
694.947	0.395	14.135	13.909
694.960	0.416	14.145	13.869
694.970	0.434	14.123	13.868
694.982	0.453	14.187	13.885
694.992	0.471	14.227	13.894
698.684	0.623	14.285	13.952
698.719	0.682	14.270	14.031
698.763	0.754	14.339	14.020
698.792	0.804	14.337	14.068
698.898	0.980	13.988	13.873
689.915	0.009	13.958	13.782
698.943	0.055	13.980	13.849
698.954	0.074	14.004	13.899
698.976	0.111	14.038	13.821
698.985	0.126	14.042	13.835
699.685	0.291	14.024	13.827
699.714	0.340	14.073	13.804
699.742	0.386	14.142	13.854
699.769	0.432	14.156	13.781
699.812	0.504	14.246	13.828
699.888	0.629		13.973
699.897	0.644	14.303	13.968
699.915	0.674	14.302	14.003
699.961	0.752	14.296	14.071
699.982	0.787	14.288	14.110
700.688	0.964	14.083	13.881
700.717	0.012	13.975	13.822
700.755	0.075	14.002	13.838
700.787	0.128	14.049	13.759
700.822	0.187	14.086	13.828
700.847	0.229	14.066	13.789
700.868	0.263	14.088	13.855
700.889	0.298	14.089	13.861
700.919	0.348	14.137	13.810
700.931	0.369	14.146	13.810
700.940	0.384	14.160	13.888
700.951	0.401	14.183	13.879
700.960	0.417	14.203	13.892
700.979	0.449	14.221	13.862

TABLE 9
J and *K* Photometry of RR Lyrae M5–V32

Geocentric Julian Date −2,447,000.0	Phase	J (mag)	K (mag)
693.681	0.583	14.472	14.185
693.761	0.759	14.475	14.171
693.806	0.858	14.594	14.368
693.842	0.937	14.450	14.348
693.872	0.000	14.086	13.952
694.669	0.742	14.480	14.164
694.697	0.802	14.414	14.079
694.731	0.877	14.696	14.363
694.765	0.953	14.392	14.166
694.803	0.036	14.078	13.999
694.853	0.145		13.860
698.658	0.455	14.397	14.055
698.690	0.525	14.401	14.193
698.728	0.610	14.442	14.231
698.769	0.699	14.516	14.152
698.827	0.825	14.529	14.184
699.659	0.643	14.451	14.145
699.692	0.716	14.426	14.110
699.721	0.778	14.437	14.223
699.749	0.840	14.511	14.236
699.784	0.916	14.429	14.357
700.665	0.839	14.499	14.034
700.696	0.908	14.506	14.105
700.732	0.986	14.021	13.901
700.763	0.053	14.114	13.946
700.801	0.138	14.047	13.954
700.830	0.200	14.112	13.951
700.853	0.250	14.102	13.932

TABLE 10
J and *K* Photometry of RR Lyrae M5–V8

Geocentric Julian Date −2,447,000.0	Phase	J (mag)	K (mag)
693.691	0.454	14.195	13.850
693.765	0.590	14.206	13.903
693.810	0.671	14.329	13.974
693.846	0.737	14.256	14.035
693.874	0.790	14.377	14.027
694.674	0.254	14.071	13.913
694.701	0.302	14.085	13.756
694.735	0.365	14.130	13.759
694.769	0.427	14.162	13.905
694.807	0.497	14.165	13.834
694.857	0.589		13.853
698.662	0.554	14.270	13.963
698.692	0.610	14.254	13.994
698.697	0.618	14.262	13.875
698.699	0.623	14.201	13.984
698.732	0.682	14.274	13.927
698.773	0.757		13.934
698.831	0.863	14.204	14.081
699.663	0.387	14.074	13.660
699.697	0.448	14.090	13.695
699.724	0.499	14.110	13.876
699.752	0.550	14.141	13.850
699.788	0.616	14.129	13.812
700.668	0.227	14.045	13.720
700.699	0.283	14.081	13.763
700.736	0.352	14.044	13.757
700.765	0.405	14.094	13.860
700.806	0.479	14.126	13.839
700.832	0.527	14.125	13.839
700.855	0.569	14.159	13.845

TABLE 11
J and *K* Photometry of RR Lyrae M5–V12

Geocentric Julian Date −2,447,000.0	Phase	J (mag)	K (mag)
693.716	0.246	14.161	13.998
693.770	0.362	14.277	14.005
693.814	0.456	14.292	14.101
693.850	0.533	14.316	14.045
693.876	0.589	14.484	14.179
694.678	0.304	14.293	13.914
694.704	0.359	14.339	13.953
694.739	0.433	14.322	14.013
694.773	0.506	14.371	14.123
694.810	0.585	14.451	14.128
694.861	0.695		14.215
698.667	0.833	14.534	14.214
698.703	0.908	14.529	14.279
698.735	0.977	13.950	13.888
698.777	0.067	14.203	13.868
698.836	0.193	14.221	13.939
699.666	0.968	14.044	13.996
699.699	0.039	14.025	13.920
699.727	0.098	14.042	13.964
699.756	0.159	14.109	13.851
699.797	0.248	14.182	13.877
700.672	0.118	14.083	13.852
700.702	0.183	14.058	13.929
700.739	0.262	14.130	13.938
700.768	0.324	14.262	13.917
700.808	0.410	14.243	13.972
700.836	0.469	14.404	14.043
700.856	0.513	14.350	14.026

TABLE 12
J and *K* Photometry of RR Lyrae M5–V59

Geocentric Julian Date −2,447,000.0	Phase	J (mag)	K (mag)
693.725	0.463	13.932	13.617
693.777	0.559	14.003	13.646
693.817	0.634	14.003	13.687
693.853	0.699	14.050	13.743
693.880	0.749	14.127	13.794
694.683	0.231	13.934	13.666
694.708	0.276	13.892	13.651
694.742	0.340	13.951	13.651
694.778	0.406	13.966	13.695
694.814	0.472	13.995	13.724
694.865	0.566		13.712
698.672	0.589	14.019	13.705
698.708	0.656	14.003	13.673
698.740	0.715	14.023	13.693
698.781	0.791	14.042	13.735
698.840	0.901	14.083	13.791
699.669	0.430	13.941	13.575
699.702	0.491	13.941	13.571
699.731	0.543	13.978	13.649
699.758	0.594	14.002	13.596
699.799	0.670	14.055	13.667
700.674	0.284	13.912	13.544
700.705	0.341	13.888	13.584
700.743	0.411	13.926	13.571
700.776	0.471	13.903	13.587
700.812	0.538	14.036	13.665
700.839	0.588	14.042	13.649
700.858	0.624	13.992	13.690

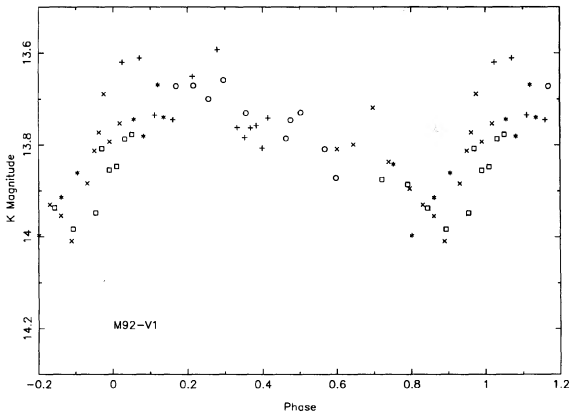

FIG. 3—The *K* band light curve for the RR Lyrae variable M92–V1 is shown as a function of phase. The different symbols denote different nights of observing.

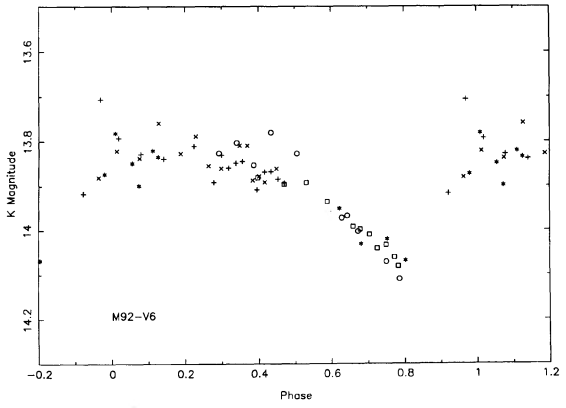

FIG. 4—The same as Fig. 3 for the RR Lyrae variable M92–V6.

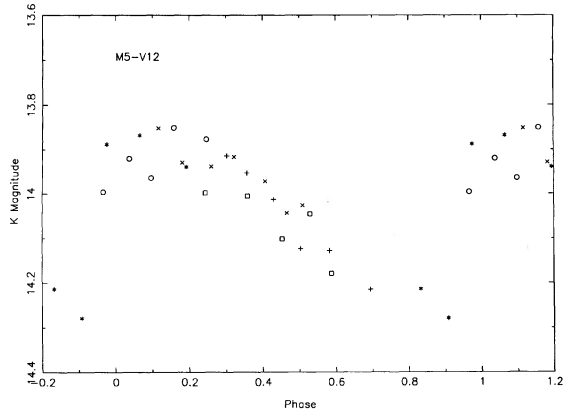

FIG. 5—The same as Fig. 3 for the RR Lyrae variable M5–V12.

Janes (1991), Carney et al. (1992), and Longmore et al. (1990), among the field RR Lyrae variables there is also a relationship between absolute K magnitude and period. It has the form (from Liu and Janes)

$$\langle M_K \rangle = -2.44(\pm 0.24)\log(P) - 0.90(\pm 0.14).$$

The observed mean K magnitudes were calculated from the K measurements from a smooth hand drawn light curve drawn through the K light curve which was digitized every 0.02 interval in phase. For M5–V32, where there were no measurements over a a significant phase interval, the K light curve of M92–V1 was used, appropriately scaled to the amplitude of the variation at K, to interpolate over the missing region. Extinction corrections at K of 0.11 A_V, where $A_V = 3.1E(B-V)$, have been applied in both clusters. Applying the extinction corrected mean K magnitudes for the six variables from Table 13 yields a distance modulus to M5 of 14.10 mag (± 0.11) (which goes up to 14.15 if M5–V59, which seems excessively bright, is omitted) and to M92 of 14.30 mag (± 0.04). These values are 0.16 ± 0.02 mag brighter than were obtained from the visual light curves. This will be discussed further in Cohen (1992).

We close with a comparison with Storm et al. For M92–V1 the agreement in $\langle K \rangle$ is very good, 13.82 versus our value of 13.80. For M5–V8 the situation is poor, and the $\langle K \rangle$ are 13.99 versus our value of 13.86. The shape of the light curve looks the same, so there may be a problem with the M5 magnitude zero point. The cause of this discrepancy is not understood.

J. G. C. is grateful to Gaston Araya Machining and to the Caltech Recycling Center for financial support. K. M. is supported by NSF Grant No. AST-8920897. We are grateful to D. Carico for help with the observing on several nights. Ben Holland helped with the observing at the 60-in. telescope.

REFERENCES

Arp, H. C. 1962, ApJ, 135, 311
Buonanno, R., Buscema, G., Corsi, C. E., Iannicola, G., Smgriglio, F., and Fusi Pecci, F. 1983, A&AS, 53, 1
Buonanno, R., Corsi, C. E., and Fusi Pecci, F. 1981, MNRAS, 196, 435
Carney, B. W., Storm, J., and Jones, R. V. 1992, ApJ, 386, 663
Carney, B. W., Storm, J., Tramell, S., and Jones, R. V. 1992, PASP, 104, 56
Cohen, J. G. 1992, ApJ, in press
Cohen, J. G. and Gordon, G. A. 1987, ApJ, 247, 869
Coutts, C. M., and Sawyer Hogg, H. 1969, Publ. David Dunlop Obs., 3, 1
Elias, J. H., Frogel, J. A., Matthews, K., and Neugebauer, G. 1982, AJ, 87, 1029
Jameson, R. F., Fernley, J. A., and Longmore, A. J. 1987, in Stellar Pulsations, ed. A. N. Cox and W. M. Starrfield, Lecture Notes in Physics, 274, 239
Jones, R. V., Carney, B. W., and Latham, D. W. 1988, ApJ, 332, 206
Kukharkin, B. V., and Kukharkina, N. P. 1980, Variable Stars, 21, 365
Liu, T. X., and Janes, K. A. 1991, The Formation and Evolution of Star Clusters, ed. K. Janes, p. 278
Longmore, A. J., Dixon, R., Skillen, I., Jameson, R. F., and Fernley, J. A. 1990, MNRAS, 247, 684
Richer, H. B., and Fahlman, G. 1987, ApJ, 316, 189
Sandage, A. R. 1990, ApJ, 350, 631
Sandage, A. R., and Walker, M. F. 1966, ApJ, 143, 313
Sawyer Hogg, H. 1973, Publ. David Dunlap Obs., 3, 1
Stetson, P. B. 1987, PASP, 99, 191
Stetson, P. B., and Harris, W. E. 1988, AJ, 96, 909
Storm, J., Carney, B. W., and Beck, J. A. 1991, PASP, 103, 1264
Thuan, T. X., and Gunn, J. E. 1976, PASP, 88, 543
Zinn, R. J. 1980, ApJS, 42, 19
Zinn, R. J. 1985, ApJ, 293, 424